Available online at www.sciencedirect.com
ScienceDirect
Journal of Organometallic Chemistry 693 (2008) 1027–1037
Journal of Organometallic Chemistry
www.elsevier.com/locate/jorganchem

Mechanistic studies on the hydrolysis of a dimeric alkylzinc bis(2-pyridylmethyl)amide

Elke Jaime [a], Alexander N. Kneifel [b], Matthias Westerhausen [b,*], James Weston [a,*]

[a] Institut für Organische Chemie und Makromolekulare Chemie, Humboldtstrasse 10, D-07743 Jena, Germany
[b] Institut für Anorganische und Analytische Chemie, August-Bebel-Str. 2, D-07732 Jena, Germany

Received 10 October 2007; received in revised form 3 December 2007; accepted 6 December 2007
Available online 15 December 2007

Abstract

Bis(2-pyridylmethyl)amine **7** reacts with selected dialkylzinc compounds to give dimeric alkylzinc bis(2-pyridylmethyl)amides **8**. Regardless of the steric bulk of the alkyl substituent, dimers with central Zn_2N_2 rings are formed. Compounds **8** undergo spontaneous hydrolysis reactions upon exposure to air/moisture which can be partially controlled if the alkyl substituent R is bulky enough [$R = CH(SiMe_3)_2$]. A dimeric compound **9** containing both zinc-alkyl substituents *and* a μ-OH functionality results. In the course of this reaction, an amide instead of the expected RH is eliminated. Extensive DFT calculations show that the facile formation of a three-centered Zn[μ-(HO···H···NHR)]Zn functionality is a crucial step. Further evidence for the importance of Zn[μ-(X···H···Y)]Zn intermediates (X, Y = O and now N) in the general mechanism of hydrolysis catalyzed by binuclear zinc compounds is thus provided.

Keywords: Alkylzinc compounds; μ-OH functionalities; Three-centered X–H–X bonds; Mechanistic studies; DFT calculations

1. Introduction

A common feature of many binuclear zinc hydrolases is the presence of a Zn–OH–Zn bridge (μ-OH functionality) in the active site [1]. The two zinc ions are usually fixed in their positions with a bridging carboxylate ligand and coordinate with either two (tetrahedral) or three (pentacoordinate) additional ligands *via* either a nitrogen or oxygen atom (N/O-coordination; Scheme 1). Although often found in biological systems, the synthesis of a binuclear zinc complex that contains a μ-OH bridge is quite demanding and there are relatively few methods for obtaining such compounds. Advances in this field have recently been summarized in two comprehensive review articles [2,3].

In the recent past, we have attempted to develop methods for synthesizing multinuclear, multifunctional zinc complexes starting from simple dialkylzinc compounds. Current progress includes a route for the synthesis of alkylzinc amides which crystallize as dimers [4,5] or trimers [6]. These can be obtained quantitatively when primary amines react with dialkylzinc compounds. However, the presence of the amide reduces the reactivity of the zinc-bound alkyl groups and a second intramolecular reaction which would result in the formation of a zinc imide does not take place since an adduct is formed instead [4,5]. Zincation of 2-pyridylmethylamine (picolylamine) yielded the corresponding alkylzinc 2-pyridylmethylamides which crystallize as either dimers or trimers depending on the size of the zinc-bound alkyl substituent [7]. The products (alkylzinc 2-pyridylmethylamides) undergo a wide spectrum of subsequent reactions which we, to date, only partially understand. These can, however, be reduced by protecting the reactive center by *N*-trialkylsilyl substitution [8]. In this case, an excess of dialkylzinc leads to an interesting oxidative C–C coupling

* Corresponding authors. Tel.: +49 (0) 3641948224; fax: +49 (0) 3641948212 (J. Weston); tel.: +49 (0) 3641948110; fax: +49 (0) 3641948102 (M. Westerhausen).
E-mail addresses: m.we@uni-jena.de (M. Westerhausen), c9weje@uni-jena.de (J. Weston).

0022-328X/$ - see front matter © 2007 Elsevier B.V. All rights reserved.
doi:10.1016/j.jorganchem.2007.12.013

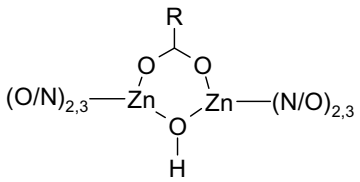

Scheme 1. Common structural motif for the active site of many binuclear zinc hydrolases.

reaction accompanied by the elimination of metallic zinc (Scheme 2) [9].

Complex **3** reacts with various proton donors in a manner that depends on the pK_a value of the protic reagent. Those less acidic than *t*-butyl amine do not react. Proteolysis with acetamide quantitatively yields 1,2-dipyridyl-1,2-bis(trialkylsilyl)ethane [10]. A primary phosphane is doubly deprotonated and, in this process, the amide ligand and the zinc-bound alkyl groups both react to form their corresponding alkanes and amines [11]. Hydrolysis with water leads to N–Si bond cleavage under formation of siloxanes. The most interesting reaction occurs with aniline. A double proton transfer under elimination of trialkylsilylamine resulted in a binuclear bis(alkylzinc) 1,2-dipyridyl-bis(phenylamido)ethane compound **5** (Scheme 3) [10]. In the case of *t*Bu

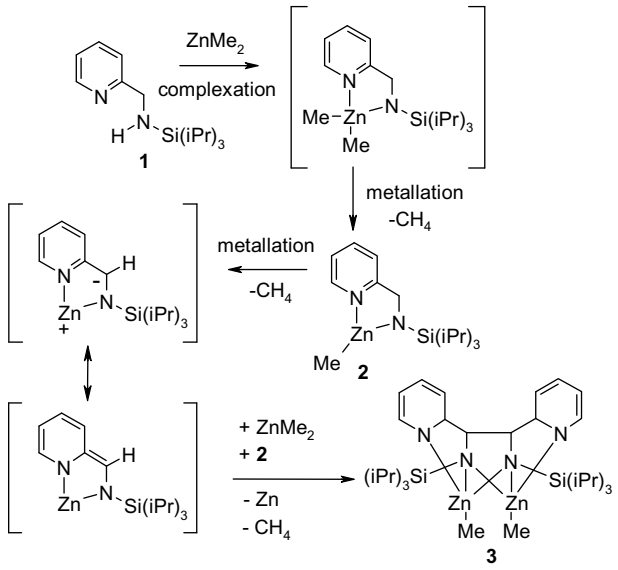

Scheme 2. Oxidative C–C coupling reaction of an alkylzinc 2-pyridylmethylamide.

substituents, dissociation into radicals *via* a hemolytic C–C bond cleavage has been reported [12].

The most common hydrolysis product of an organozinc compound is an oxygen-centered zinc tetrahedron. Compounds with this structure fragment have recently gained considerable attention since their potential as effective hydrogen storage materials has been demonstrated [13]. Controlled partial hydrolysis which would result in an alkylzinc compound with a hydroxo ligand has, on the other hand, very rarely been investigated. Mechanistic investigations on the hydrolysis of Et_2Zn using cyroscopic methods have suggested that $(EtZnOH)_2$ is an intermediate on the way to formation of $EtZn(OZn)_3OH$ [14]. The half life of EtZnOH had been determined earlier by IR spectroscopy and ethane evolution to be 6 min in wet glyme at 30 °C [15]. Due to the high reactivity of alkylzinc hydroxides towards further alkane elimination, only recently are examples slowly being reported. For example, the metathesis reaction of $(Me_2PhSi)_3C$–ZnCl with NaOH yields $[(Me_2PhSi)_3C–Zn(\mu\text{-}OH)]_2$ and, due to the kinetic stabilization provided by the bulky substituents, a solid state structure of this compound could be determined [16].

We have recently become interested in the reaction of tridentate amine ligands such as **7** (Scheme 5) with alkylzinc compounds in the hope of obtaining stable dinuclear zinc complexes which can be hydrolyzed in a controlled manner to yield alkylzinc hydroxides with a binuclear μ-OH bridge. During the course of writing up our results, two independent groups have also reported first results in this area. Jana et al. reported that the controlled oxygenation of simple alkylzinc compounds with and without the presence of small amounts of water lead to different product mixtures (mono or bis cubane structures containing both Zn–R and μ-OR bridges) [17]. More relevant to our work is the successful synthesis and structural characterization of the *N*-heterocyclic carbene stabilized organozinc hydroxide **6** (Scheme 4) recently reported by Ananthar-aman and Elango [18].

2. Results and discussion

2.1. Synthesis and characterization of dimeric alkylzinc bis(2-pyridylmethyl)amides 8

The amides **8** with R = Me (**8a**) [19] and $CH(SiMe_3)_2$ (**8b**) were easily accessible by the zincation of $HN(CH_2py)_2$ (**7**) with ZnR_2 in toluene (Scheme 5). Regardless of the ste-

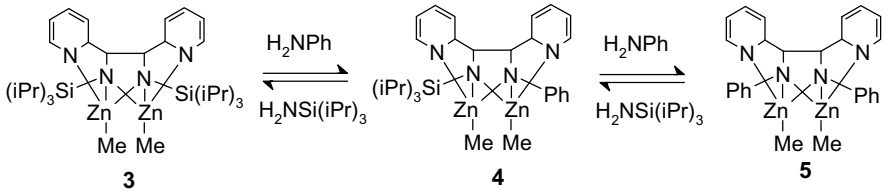

Scheme 3. Reaction of aniline with **3** to form **5** under elimination of trialkylsilylamine.

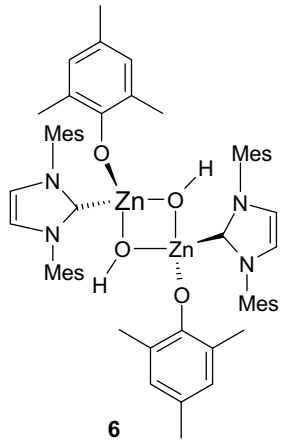

6

Scheme 4. A recent success in obtaining an organozinc hydroxide.

ric bulk of the alkyl substituent, dimers with central Zn_2N_2 rings were formed. Addition of the Lewis base THF did not lead to the formation of monomers; an X-ray analysis of **8a** showed that THF co-crystallized between the dimers without significant contacts to the zinc ions.

Both dimers are centrosymmetric in the solid state and only one pyridyl group of each ligand is coordinated to zinc (Fig. 1; Table 1 contains selected structural data). The endocyclic Zn1–N2 and Zn1–N2′ bond lengths in both dimers are somewhat shorter than the exocyclic Zn–$N_{pyridyl}$ bonds due to an additional electrostatic attraction between the amido group and the zinc cation. The larger steric demand of the bis(trimethylsilyl)methyl group in **8b** and the α-silyl effect lead to shorter endocyclic bond lengths as compared to **8a**. Due to the expanded coordination sphere of zinc, the Zn1–C13 bonds in **8a** (199.0 pm) and **8b** (199.4 pm) are slightly (although not uncharacteristically) longer than that observed for dimethylzinc (195.5 pm) [20]. This lengthening is also observed for the Zn–$C_{carbene}$ bond in compound **6** (203.9 ppm) [18]. Perhaps the most unusual feature in **8b** is the presence of quite short C13–Si bonds as a consequence of the α-silyl effect (177.0 and 179.7 pm).

2.2. Partial hydrolysis of *8*

The reaction of **8a** with water was quite violent and resulted in complete decomposition. Addition of water to the sterically more shielded complex **8b** either as a toluene solution or as water vapor also resulted in decomposition under formation of numerous products that have not yet

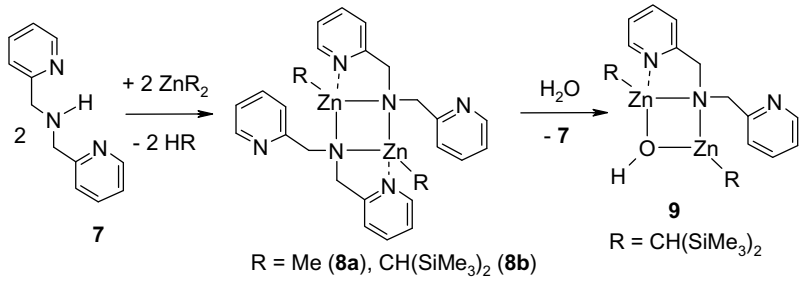

Scheme 5. Synthesis of the dimeric alkylzinc bis(2-pyridylmethyl)amides **8a/b** and the partial hydrolysis of **8b** to form **9**.

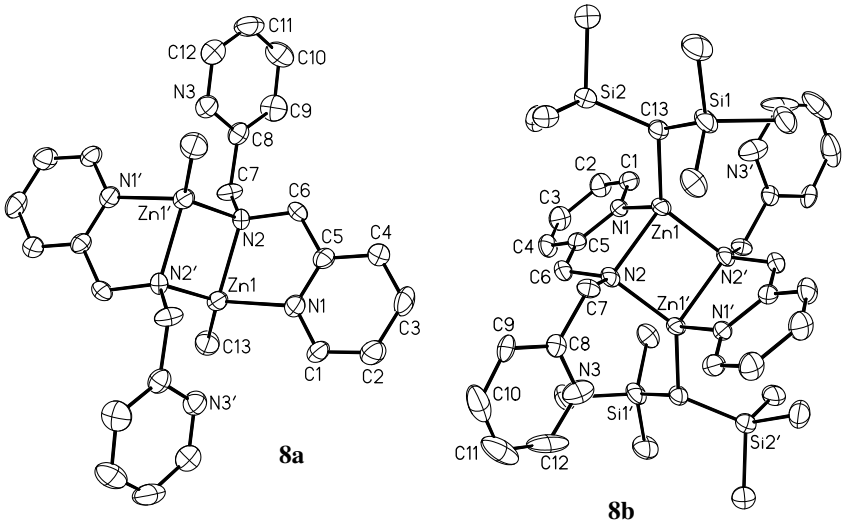

Figure 1. Molecular structures (X-ray analysis) of **8a** and **8b**. The hydrogen atoms as well as the THF molecule in **8a** (co-crystallizes between the dimeric units) are omitted for clarity. Symmetry related atoms ($-x$, $-y$, $-z$) are marked with an apostrophe. The ellipsoids represent a probability of 40%. Selected structural data can be found in Table 1.

Table 1
Selected bond lengths (pm) of **7a**, **7b** and **8** as well as relevant data for compound **6** [18]

	8a · THF	8b	9	6
Zn1–N1	217.6(6)	207.8(6)	212.3(2)	193.3(3)[a]
Zn1–N2	210.3(5)	203.7(5)	207.2(2)	–
Zn1–O	–	–	200.7(2)	198.2(3)
Zn1–C13	199.0(8)	199.4(8)	200.5(2)	203.9(4)[b]
Zn1′/Zn2–N2	206.8(5)	202.7(6)	207.9(2)	–
Zn2–N3	–	–	218.1(2)	–
Zn2–O	–	–	200.6(2)	197.3(3)
Zn2–C20	–	–	199.7(2)	–
Si1–C13	–	177.0(8)	183.2(2)	–
Si2–C13	–	179.7(8)	185.1(2)	–
N1–C1	134.9(8)	129(1)	134.7(3)	–
N1–C5	134.0(8)	131.3(8)	134.1(3)	–
C1–C2	136(1)	133(1)	137.1(3)	–
C2–C3	139(1)	135(1)	137.6(4)	–
C3–C4	136(1)	131(1)	138.1(4)	–
C4–C5	138(1)	132(1)	139.0(3)	–
C5–C6	152(1)	146(1)	150.5(3)	–
N2–C6	144.6(9)	141.4(8)	146.0(3)	–
N2–C7	147.3(9)	142(1)	146.5(3)	–
C7–C8	151(1)	147.1(9)	150.2(3)	–
C8–C9	138(1)	132(1)	138.1(3)	–
C9–C10	139(1)	133(1)	137.9(4)	–
C10–C11	138(1)	127(2)	137.9(4)	–
C11–C12	136(1)	129(2)	137.3(4)	–
N3–C8	136.0(9)	133(1)	134.2(3)	–
N3–C12	135.3(9)	135(1)	134.2(3)	–
Zn1···Zn1′/Zn2	293.7(2)	285.6(2)	288.09(3)	297.32(8)

[a] Zn–O (2,4,6-trimethylphenolate) bond length.
[b] Zn–$C_{carbene}$ bond length.

been fully characterized. However, exposure of a concentrated toluene solution to air led to a slow hydrolysis reaction (Scheme 5) under deposition of a few crystals of the hydroxide complex **9**. Quite surprisingly, an amide was eliminated in the course of the hydrolysis instead of an alkyl group. Due to the immediate crystallization of **9**, subsequent decomposition reactions were slowed down. The crystals thus obtained were coated with bis(2-pyridylmethyl)amine and therefore no reliable yields and melting points for this compound can be given. An X-ray analysis of **9** (Fig. 2) confirmed the presence of a μ-OH functionality. Whereas the Zn–C bond lengths in **9** remain unchanged as compared to **8b**, the Zn–N bonds are longer due to the higher intramolecular electrostatic repulsion. The hydroxo group is shielded by the bis(trimethylsilyl)methyl substituents which effectively prevents oligomerization *via* hydrogen bridges. The non-bonding transannular Zn···Zn contact correlates with the Zn–N distances.

The three compounds reported in this article allow for a direct comparison of the effect of pyridyl group coordination to zinc, substitution of the zinc-bound methyl group with a trimethylsilyl substituent as well as the influence of the hydroxo anion on the structural parameters (Table 1). In all of these compounds, the zinc atoms are in a distorted tetrahedral environment and are bound to an alkyl group, an amido and a pyridyl ligand. The fourth substituent is either an amido (**7a** and **7b**) or a hydroxo anion (**8**).

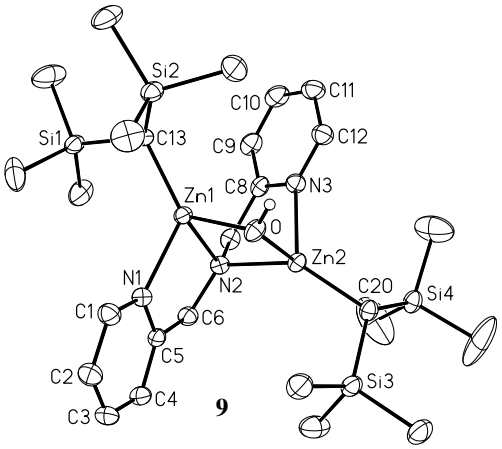

Figure 2. Molecular structure (X-ray analysis) of **9**. The hydrogen atoms with the exception of the hydroxo group are omitted for clarity. The ellipsoids of all non-hydrogen atoms represent a probability of 30%. Selected structural data can be found in Table 1.

In $[(Me_2PhSi)_3C–Zn(\mu\text{-}OH)]_2$ which, until the study of Anantharaman and Elango [18], was the only known example of a compound containing alkylzinc units connected by hydroxo groups, the zinc atoms are in a distorted trigonal planar environment with Zn–C and Zn–O bond lengths of 195.3(7) and 189.9(9) pm, respectively [16]. Due to the higher coordination number of the zinc atoms in compounds **8**, the Zn–C and Zn–O bonds are somewhat elongated as compared to $[(Me_2PhSi)_3C–Zn(\mu\text{-}OH)]_2$. These values are quite comparable to those found in compound **6**.

2.3. NMR-investigations on 8 and 9

Although $[(Me_2PhSi)_3C–Zn(\mu\text{-}OH)]_2$ can be prepared from alkylzinc chloride and NaOH in a straightforward procedure [16], it is quite difficult to isolate and investigate since it is very sensitive towards moisture and hydrolyzes under formation of a multitude of side products. Compounds **8a/b** and **9** proved to be somewhat less sensitive and we succeeded in obtaining NMR-spectra.

In solution (C_6D_6), exchange between the coordinated pyridyl arm of the ligand and the free pendent sidearm is fast on the NMR time scale for compounds **8** which resulted in averaged signals for the aromatic ligands (Table 2). It is quite remarkable that the averaged ^1H and ^{13}C shifts for **8a/b** do not differ significantly from those observed for the pyridyl units of **9** in which both are attached to the zinc ions. The greatest difference between the spectra of the amides (**8a/b**) and the μ-OH compound **9** is observed for the chemical shift of the zinc-bound alkyl group. This signal is shifted slightly downfield (3.6 ppm) in the ^{13}C NMR spectrum and a remarkable high field shift of over 1.2 ppm occurs in the ^1H NMR spectrum.

3. Mechanism of hydrolysis

The formation of **9** under loss of an amide ligand instead of the zinc-bound alkyl group is quite unusual.

Table 2
NMR chemical shifts (ppm) measured in C_6D_6 at 30 °C for compounds **8a**, **8b** and **9**

δ	**8a** · THF	**8b**	**9**
^{1}**H**			
Pyr 1	8.47	8.17	8.46
Pyr 2	6.47	6.54	6.62
Pyr 3	6.92	6.95	7.08
Pyr 4	6.84	6.75	7.08
CH_2	4.24	4.25	3.91
ZnCH/Me	−0.28	−0.03	−1.28
$SiMe_3$	–	0.10	0.29, 0.10
^{13}**C**			
Pyr 1	148.2	147.0	149.2
Pyr 2	121.1	122.8	121.7
Pyr 3	136.1	138.1	135.7
Pyr 4	121.9	122.6	121.4
Pyr 5	164.0	160.6	160.6
CH_2	60.8	59.6	54.9
ZnC	−17.1	−2.5	1.1
$SiMe_3$	–	4.4	4.4
^{29}**Si**	–	−1.3	−1.3

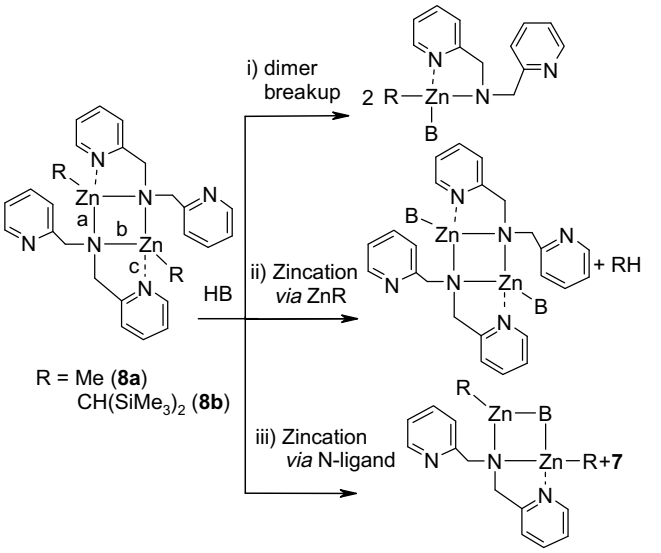

Scheme 6. Mechanistic possibilities for the initial step in the hydrolysis mechanism of **8a**/**8b**.

Most alkylzinc complexes would have instead eliminated an alkane on the way towards generating an oxygen-centered zinc tetrahedron. Furthermore, **9** (and **6** [18]) are the first examples of compounds that contain a μ-OH functionality as well as a zinc-bound alkyl group that in addition to their mere existence, are stable enough for mechanistic investigations.

Each of these nucleophilic functionalities is extremely important in its own right. Ever since the discovery of Et_2Zn by Frankland in 1894 [21], dialkyl zinc compounds are well known, widely used alkylating reagents in synthetic chemistry. Long considered to be biologically irrelevant, zinc promoted alkyl transfer reactions have recently been identified in the active sites of certain alkyltransferases [22]. However, the general role of zinc in biochemical processes is to promote the enzymatic hydrolysis of peptide and phosphate ester bonds, often via a bimetallic active site containing a Zn(μ-OH)Zn unit [2,3]. On the synthetic side of things, the enormous potential of a β-amino alcohol catalyzed reduction of a carbonyl compound with a dialkyl zinc compound (Noyori reaction) is well recognized [23]. This reaction is known to proceed over a catalytic active intermediate containing a Zn(μ-OR)Zn functionality.

We are currently undertaking a joint experimental–theoretical investigation with the intent of providing information on the relative reactivity of these potent nucleophiles and now report our first results. There are several mechanistic possibilities for the initial reaction of **8a**/**b** with a Brønsted base HB (water or amine, for example) which are illustrated in Scheme 6. These include (i) breakup of the dimer into monomers with coordination of the neutral Brønsted base B to the zinc ions, (ii) zincation mediated by the zinc-bound alkyl groups under elimination of RH or (iii) zincation via a zinc-bound amide ligand.

3.1. Possibility of dimer breakup (i)

There is no indication in NMR experiments for an equilibrium between monomeric and dimeric forms of **8a** or **8b** – even after addition of the Lewis base THF. As already has been discussed, THF does not interact with **8a** in the solid state; it co-crystallizes between the dimeric units. Furthermore, calculation of the thermodynamic equilibrium [**8a**(dimer) + 2 THF $\rightleftharpoons$ **8a**(monomer) · THF] at the B3LYP/lanl2dz level of theory revealed that this step is quite endothermic ($\Delta G = +18.6$ kcal/mol). If the Brønsted base water is used in the calculations instead of THF, it reacts via an amide ligand mediated zincation (discussed below). A stationary point for a water mediated breakup of **8a** could not be found on the B3LYP/lanl2dz hypersurface. Both experimental and theoretical findings thus conclude that this possibility can essentially be ruled out as a viable first step in a hydrolysis mechanism.

3.2. Possibility of zincation mediated by the zinc-bound alkyl groups (ii)

Considering only the relative acidities of a zinc alkyl substituent and a μ-OH group, one would predict that this mechanistic possibility should be clearly favored. However, in spite of extensive calculations at the B3LYP/lanl2dz level of theory on **8a**, we did not succeed in finding a *single* reaction pathway on the hypersurface for this mechanistic possibility. The most obvious reason for this is the immediate generation of a three-center Zn–O···H···N–Zn bridge upon approach of the water which leads to a clear preference for reaction with the amide ligand (discussed below).

Three-centered Zn–O···H···O–Zn bridges can be quite easily generated by hydration of a μ-OH functionality as has been extensively investigated by Meyer et al. who have also succeeded in demonstrating that the reactivity of binu-

clear zinc complexes can be enhanced due to bridge formation [24]. A complex containing a Zn(μ-OH)Zn bridge, for example, is unreactive towards CO_2 whereas the water adduct with a Zn[μ-(HO···H···OH)]Zn functionality immediately forms a carbonate [25]. A detailed theoretical investigation confirmed an intrinsic activation of a μ-OH bridge upon "hydration" [26]. Formation of a zinc-bound "H_3O_2"-functionality is also discussed as being an important activation step in the mode of action of bimetallo zinc-based hydrolases [27,28].

3.3. Possibility of zincation mediated by the zinc-bound alkyl groups (iii)

Of all three mechanistic possibilities, this step is the only viable one according to our calculations. With an overall exothermicity (ΔG) of −25.5 kcal/mol and rather low activation barriers (the largest is 13.7 kcal/mol), this reaction can be expected to occur spontaneously upon addition of water to **8a**. As a water approaches **8a**, it first builds an encounter complex on the periphery and then inserts itself into a Zn–N bond under generation of an intermediate with a three-center Zn–O···H···N–Zn functionality. Since there are three different Zn–N bonds in **8a** (a, b and c in Scheme 6), there are three different pathways on the hypersurface for the attack of water. All are viable mechanisms for **8a** and are illustrated in Schemes 7, 8 and 9 and Fig. 3. To clearly illustrate the different reaction steps, chemical drawings have been employed; the calculated structures of each intermediate/transition structure can be found in Supplementary material (Schemes S1, S2 and S3). The energies (ΔG values) of the different species on the hypersurface relative to **8a** can be found in Table 3.

3.3.1. Pathway a: attack on the Zn1–N2′ bond

If a water comes into contact with a free pyridyl arm, it forms a strong hydrogen bond with the aromatic nitrogen (encounter complex **Ea1** in Scheme 7) which optimally positions it for an attack on the Zn1–N2′ bond over **Ta1** ($\Delta G = +8.0$ kcal/mol; rate determining step). In this transition structure, a Zn1–O bond is being formed while the Zn1–N2′ bond is broken. At the same time, a proton from water is being transferred to the amido group (N2′) with the help of the pyridyl arm. An exergonic ($\Delta G = -12.6$) intermediate **Ia1** with a Zn–O···H···N–Zn functionality is generated which then reacts further over **Ta2** to generate a μ-OH functionality (intermediate **Ia2**). At this point, the amide ligand (**7**) is bound only by a Zn-pyridyl contact and an OH···N hydrogen bond. The free pyridyl arm on the ligand still connected to both zinc ions then moves in and displaces the amide ligand over **Ta3**. A loosely bound encounter complex **ECa2** is formed before the amide ligand finally departs leaving compound **9** behind. The total reaction is with $\Delta G = -25.5$ kcal/mol quite exergonic (see Table 3).

3.3.2. Pathway b: attack on the Zn1–N2 bond

Alternatively, if a water molecule approaches the Zn1–N2 bond, it first comes in contact with the hydrogen atoms of the two methylene linker units in the amido ligand (forms encounter complex **Eb1**). From this position it can attack the Zn1–N2 bond over **Tb1** (rate determining step; $\Delta G = +13.7$ kcal/mol). In this transition structure an intermediate **Ib1** with a Zn–O···H···N–Zn functionality is being formed. The oxygen atom in this three-center bond then attacks zinc to generate a μ-OH group. The former amino nitrogen is protonated in this step (**Tb2**;

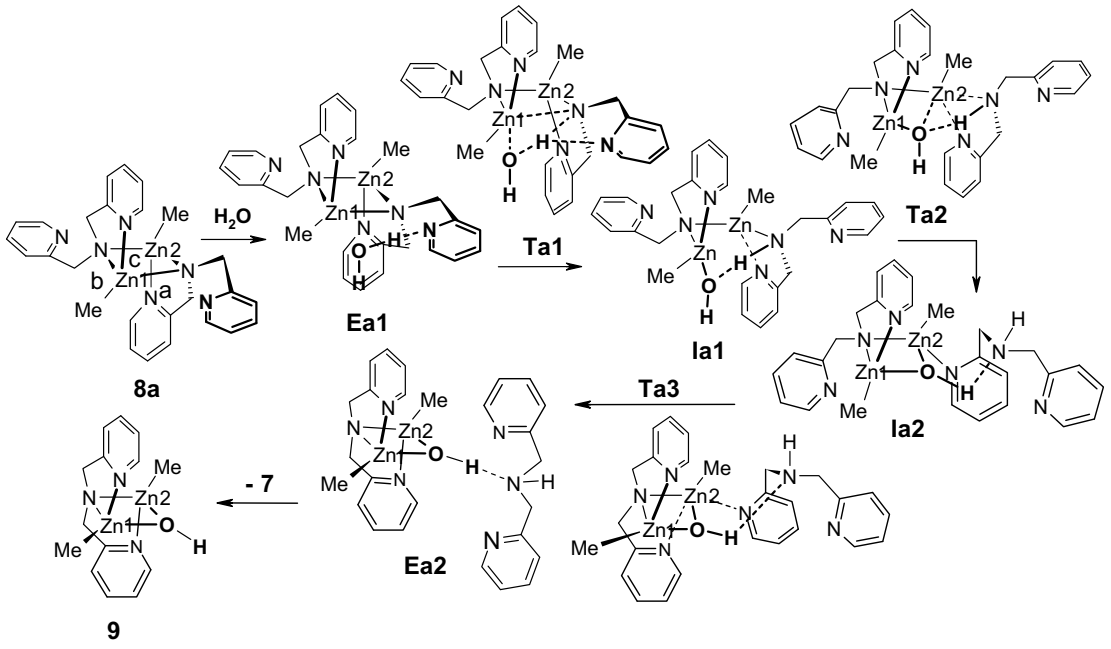

Scheme 7. Pathway a – attack of water on the Zn1–N2′ bond in **8a**. Calculated at the B3LYP/lanl2dz level of theory.

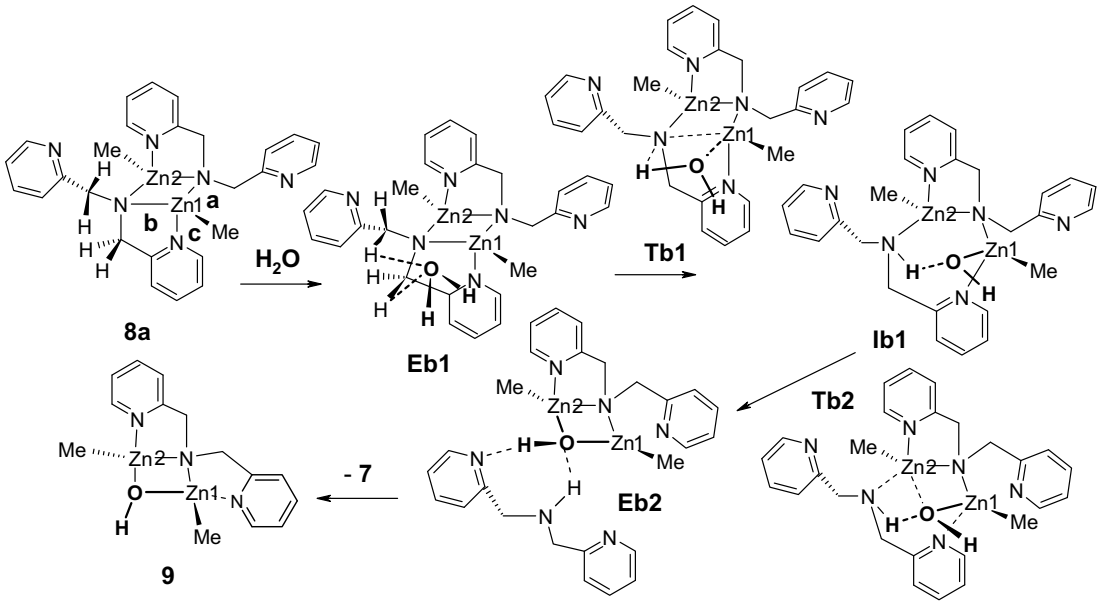

Scheme 8. Pathway b – perspective has been rotated as compared to Scheme 7 for better illustration of the reaction mechanism. Calculated at the B3LPY/lanl2dz level of theory.

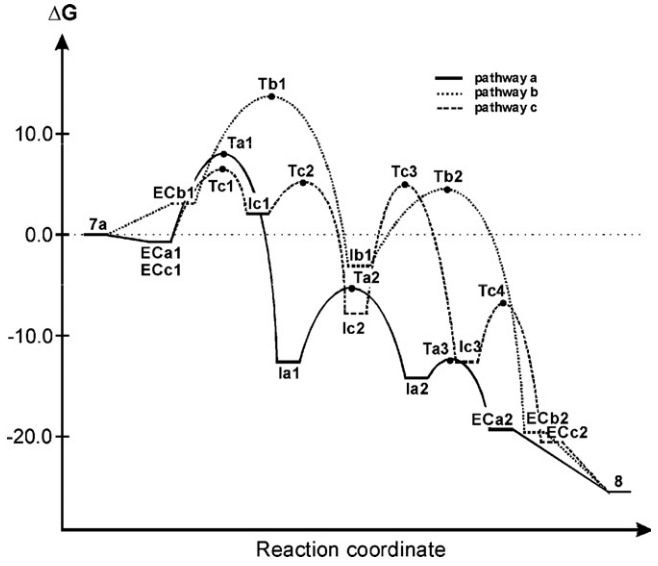

Figure 3. Energy diagram of the pathways a, b and c for the zincation via N-ligand. Calculated at the B3LYP/lanl2dz level of theory and given in kcal/mol relative to **8a** and a free water molecule.

Table 3
Gibb's free energies of reaction (kcal/mol) for the reaction pathways **a**, **b** and **c**. Calculated at the B3LYP/lanl2dz level of theory and given relative to **8a** and a free water molecule

	ΔG (x = a)	ΔG (x = b)	ΔG (x = c)
8a	0.0	0.0	0.0
Ex1	−0.7	+3.1	−0.7
Tx1	+8.0	13.7	+6.4
Ix1	−12.6	−3.1	+2.1
Tx2	−5.3	+4.5	+5.2
Ix2	−14.2	–	−7.8
Tx3e	−12.3	–	+5.0
Ix3	–	–	−12.6
Tx4	–	–	−6.7
ECx2	−19.3	−19.6	−20.6
9	−25.5	−25.5	−25.5

$\Delta G = +4.5$ kcal/mol) by a hydrogen atom originating from the water molecule while the free pyridyl arm moves in and displaces the amide ligand (**7**). A loosely bound encounter complex **Ea2** is formed before the amide ligand **7** finally departs leaving compound **9** behind.

3.3.3. Pathway c: attack on the Zn1–$N_{pyridyl}$ bond

The insertion of water into the Zn2–$N_{pyridyl}$ bond has the lowest barrier of all pathways (see Scheme 9). In addition, it is also the most complex reaction pathway on the hypersurface. In the initial step, the free pyridyl arm captures a water molecule via the formation of a hydrogen bond to the ring nitrogen (encounter complex **Ec1** is generated; $\Delta G = -0.7$ kcal/mol). The ring nitrogen in the pyridyl arm bound to Zn1 then helps to pull the water into electrostatic range of the *o*-hydrogen of the aromatic ring (transition structure **Tc1;** $\Delta G = +6.4$ kcal/mol) which then promptly forms a second stabilizing hydrogen bond to the water (intermediate **Ic1**). The transition structure leading to the formation of **Ic1** is the rate limiting step – and furthermore possesses the lowest overall barrier of all three pathways. The metastable intermediate **Ic1** ($\Delta G = +2.1$ kcal/mol) then stabilizes itself via ligand exchange at Zn1 (water for $N_{pyridyl}$) over the pentacoordinated transition structure **Tc2** to form the exergonic intermediate **Ic2** ($\Delta G = -7.8$ kcal/mol). The zinc-bound water then inserts itself into the N1–Zn2 bond over **Tc3** to generate **Ic3** ($\Delta G = -12.6$ kcal/mol) which is characterized by a six-membered ring containing a three-center Zn–O···H···N–

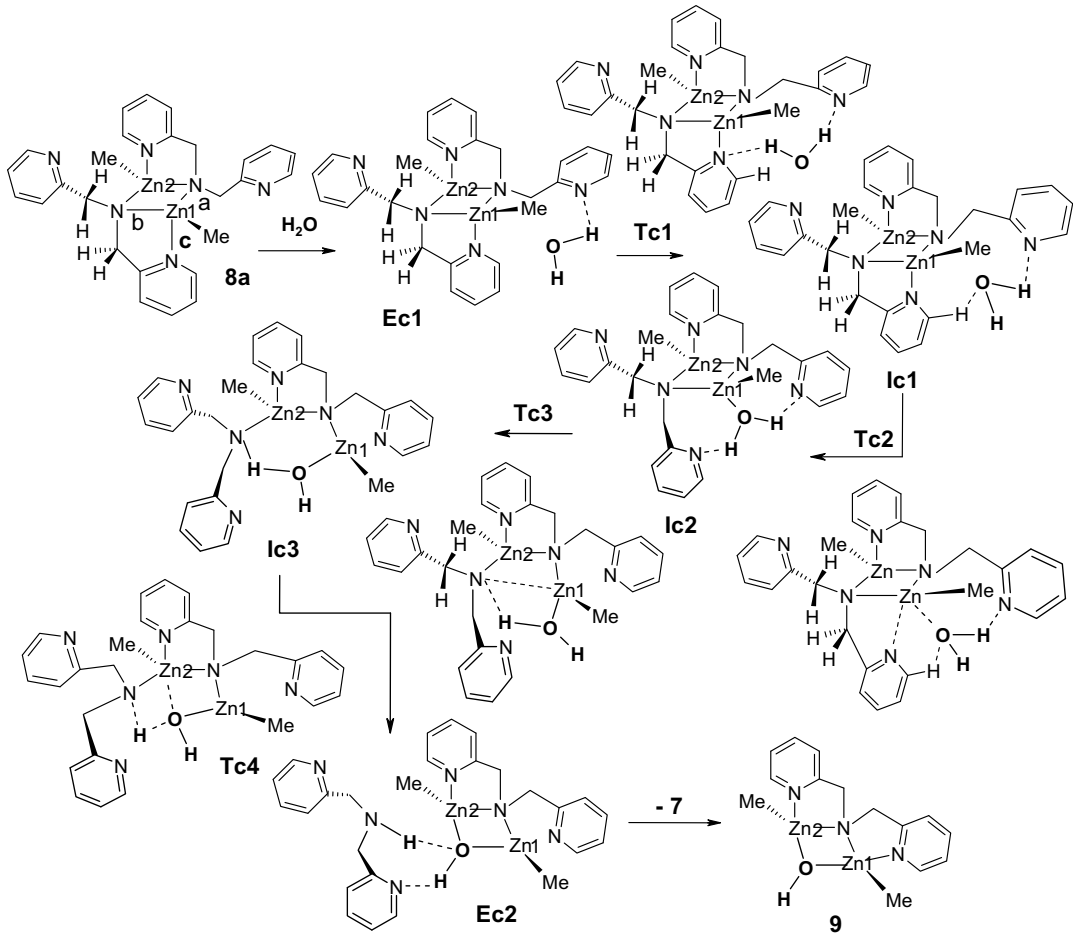

Scheme 9. Pathway c – perspective has been rotated as compared to Scheme 7 for better illustration of the reaction mechanism. Calculated at the B3LYP/lanl2dz level of theory.

Zn bond. The oxygen in the three-centered bond then swings in over **Tc4** and complexes with Zn2 under regeneration of a four-membered ring system. At the same time, the N–Zn2 contact is given up. The resulting amine **7** then departs over encounter complex **Ec2**.

All reaction steps are plausible for R = methyl (compound **8a**). We do not know how this will change as steric bulk increases. There will definitely be an effect since the hydroxo complex can be obtained with $SiMe_3$ but not for methyl. We are now investigating this case.

4. Conclusions

The calculations were performed on compound **8b** (R = Me) and match the experimental results (uncontrolled hydrolysis) quite satisfactorily since the lowest activation barrier (pathway c) is only 6.4 kcal/mol. As the steric bulk increases, the barrier obviously increases since hydrolysis of **8b** [$R = CH(SiMe_3)_2$] can be experimentally controlled to some degree. We are now investigating the effect of steric bulk on the hypersurface as well as analyzing electronic effects in the transition structures (rate controlling steps) with the aim of finding a way to slow down the reaction a bit more with the goal of obtaining a palette of binuclear zinc compounds containing both zinc-alkyl and μ-OH functionalities.

5. Computational details

All calculations reported in this article were performed with the gradient-corrected hybrid B3LYP [29] density functional using the GAUSSIAN 03 [30] program package. The lanl2dz basis set (D95 [31] basis for the first row atoms and the Los Alamos effective core potential for the zinc ions [32]) was employed throughout since extensive calculations on similar binuclear zinc complexes have clearly demonstrated that this medium-sized basis set delivers qualitatively and quantitatively similar results as the much larger aug-cc-Pvtz [33] basis [26,27]. All species found on the hypersurface were characterized as energetical minima or transition structures via vibrational analyses. Default convergence criteria were used and no symmetry was employed in any of the calculations. All relative stabilities reported are gas phase Gibb's free energies that contain standard thermochemical (298 K) and vibrational corrections.

6. Experimental

6.1. General remarks

All reactions were performed in an argon atmosphere using standard Schlenk techniques. All solvents were dried and thoroughly deoxygenated according to standard procedures prior to use. The NMR data are listed in Table 2. IR spectra were recorded using Nujol suspensions between KBr windows. The starting materials $Zn[CH(SiMe_3)_2]_2$ [34] and $[MeZnN(CH_2py)_2]_2$ [19] were prepared by known procedures.

6.2. Synthesis of $[MeZn\{\mu\text{-}N(CH_2py)_2\}\cdot THF]_2$ (**8a** · THF)

Bis(2-pyridylmethyl)amine **7** (3.6 ml, 20.0 mmol) was dissolved in 20 ml of toluene and cooled to 0 °C upon which 10 ml of a solution of 2.0 M dimethylzinc in toluene (20.0 mmol) were added dropwise. After complete addition, the solution was warmed to r.t. and stirred for an additional 10 h. The volume of the solution was reduced to a few milliliters and 1.5 ml of THF was added. Cooling of this solution to −20 °C led to the precipitation of colorless crystals of $[MeZn\{\mu\text{-}N(CH_2py)_2\}\cdot THF]_2$ (**8a** · THF). NMR data showed that the crystal contained THF and that the solution contained $[MeZnN(CH_2py)_2]_2$ rather than a monomeric THF complex. To support these findings, the crystal structure was determined. These crystals became dull immediately due to loss of THF and no melting point of the THF adduct was determined. After drying in vacuum, the THF-free compound showed a melting point of 126 °C. The physical data are in agreement with the literature data [19].

6.3. Synthesis of $[(Me_3Si)_2CHZn\{\mu\text{-}N(CH_2py)_2\}]_2$ (**8b**)

Bis(2-pyridylmethyl)amine (0.12 ml, 0.70 mmol) was dissolved in 3 ml of toluene and added dropwise to a solution of 0.22 g of $Zn[CH(SiMe_3)_2]_2$ (0.70 mmol) in 3 ml of toluene. This solution was stirred for 10 h. Thereafter, the volume was reduced to 3 ml. At 5 °C 0.09 g of colorless crystals of **8b** (0.1 mmol, 30%) precipitated. M.p. 149 °C. IR: 3063 m, 3011 m, 2945 vs, 2894 s, 2821 m, 1654 vw, 1605 s, 1592 vs, 1570 vs, 1474 s, 1457 s, 1434 vs, 1356 w, 1344 w, 1285 m, 1240 vs, 1148 m, 1127 m, 1101 m, 1048 s, 1028 s, 1023 s, 995 s, 966 w, 852 vs, 836 vs, 756 vs, 679 m, 668 m, 642 w, 627 w, 614 w, 609 w, 592 vw, 490 w, 404 m. MS (CI+, *iso*-butane, *m/z*): 422 ($M^+_{monomer}-H$). Elemental *Anal.* Calc. for ($[C_{19}H_{31}N_3Si_2Zn]_2$, 846.06): C, 53.94; H, 7.39; N, 9.93. Found: C, 53.65; H, 7.41; N, 9.86%.

6.4. Synthesis of $[\{(Me_3Si)_2CHZn\}_2(\mu\text{-}OH)\text{-}\{\mu\text{-}N(CH_2py)_2\}]$ (**9**)

The mother liquor after collecting the crystals of **2** was concentrated till the residue was slightly oily. The stopcock was then removed for 10 min to allow contact with air.

Table 4
Crystal data and refinement details for the X-ray structure determinations

Compound	**8a** · **THF**	**8b**	**9**
Formula	$C_{17}H_{23}N_3OZn$	$C_{38}H_{62}N_6Si_4Zn_2$	$C_{26}H_{51}N_3OSi_4Zn_2$
Fw (g mol^{-1})	350.75	846.08	664.80
T (°C)	−80(2)	−80(2)	−73(2)
Crystal system	Monoclinic	Monoclinic	Triclinic
Space group	$P2_1/n$	$P2_1/c$	$P\bar{1}$
a (Å)	12.4017(15)	11.502(3)	8.5984(2)
b (Å)	7.4016(8)	11.787(3)	11.2089(2)
c (Å)	18.4205(18)	14.934(4)	19.7679(4)
α (°)	90.00	90.00	86.8323(12)
β (°)	97.315(4)	100.666(4)	78.1016(12)
γ (°)	90.00	90.00	71.1091(9)
V (Å^3)	1677.1(3)	1989.7(8)	1763.72(6)
Z	4	2	2
ρ (g cm^{-3})	1.389	1.412	1.252
μ (cm^{-1})	14.69	13.62	15.17
Measured data	5730	8412	17255
Data with $I > 2\sigma(I)$	1608	2300	5362
Unique data (R_{int})	2405	2790	6123
wR_2 (all data, on F^2)[a]	0.1332	0.1640	0.0725
R_1 ($I > 2\sigma(I)$)[a]	0.0634	0.0610	0.0278
s[b]	1.066	1.034	1.030
Residual density (e Å^{-3})	0.416/ − 0.731	0.568/ − 0.811	0.373/ − 0.317
Absorption method	SADABS	SADABS	SADABS
Absorption corr. T_{min}/T_{max}	0.711/1.0	0.495/1.0	0.722/1.0
CCDC No.	CCDC 620312	CCDC 620311	CCDC 620310

[a] Definition of the R indices: $R_1 = (\Sigma||F_o| - |F_c||)/\Sigma|F_o|$, $wR_2 = \{\Sigma[w(F_o^2 - F_c^2)^2]/\Sigma[w(F_o^2)^2]\}^{1/2}$ with $w^{-1} = \sigma^2(F_o^2) + (aP)^2$.
[b] $s = \{\Sigma[w(F_o^2 - F_c^2)^2]/(N_o - N_p)\}^{1/2}$.

Within a few days colorless crystals precipitated in the oil which were suitable for X-ray diffraction experiments. The residue contained compounds **8b**, **9** and $HN(CH_2py)_2$ in addition to other products. It was not possible to remove the oil which coated the isolated crystals. Therefore no melting point or elemental analysis is given. Estimated yield of **9**: 5%. IR: $\nu(OH) = 3312\ cm^{-1}$.

6.5. Crystal structure determinations

Data were collected on a Siemens P4 diffractometer with CCD area detector with graphite-monochromated Mo Kα radiation using oil-coated rapidly cooled single crystals. All structures were solved by direct methods and refined using the software package SHELXL-97 [35]. Neutral scattering factors were taken from Cromer and Mann [36] and for the hydrogen atoms from Stewart et al. [37]. The non-hydrogen atoms were refined anisotropically. The H atoms were considered with a riding model under restriction of ideal symmetry at the corresponding carbon atoms, however, the O-bound hydrogen atom was refined isotropically. Crystallographic parameters, details of data collection and refinement procedures are summarized in Table 4.

Acknowledgements

Financial support by the Deutsche Forschungsgemeinschaft (Collaborative Research Initiative 436, Jena, Germany) and the Thüringer Ministerium für Wissenschaft, Forschung und Kunst (Erfurt, Germany) is gratefully acknowledged.

Appendix A. Supplementary material

CCDC 620312, 620311 and 620310 contains the supplementary crystallographic data for **8a** · **THF**, **8b** and **9**. These data can be obtained free of charge from The Cambridge Crystallographic Data Centre via www.ccdc.cam.ac.uk/data_request/cif. Furthermore, calculated structures at the B3LYP/lanl2dz level of theory for the hydrolysis pathways (Schemes S1–S5) are available. Supplementary data associated with this article can be found, in the online version, at doi:10.1016/j.jorganchem.2007.12.013.

References

[1] (a) W.T. Lowther, B.W. Matthews, Chem. Rev. 102 (2002) 4581;
(b) N. Sträter, W.N. Lipscomb, T. Klabunde, B. Krebs, Angew. Chem., Int. Ed. Engl. 35 (1996) 2024;
(c) W.N. Lipscomb, N. Sträter, Chem. Rev. 96 (1996) 2375;
(d) D.E. Wilcox, Chem. Rev. 96 (1996) 2435.
[2] G. Parkin, Chem. Rev. 104 (2004) 699.
[3] J. Weston, Chem. Rev. 105 (2005) 2151.
[4] M.M. Olmstead, W.J. Grigsby, D.R. Chacon, T. Hascall, P.P. Power, Inorg. Chim. Acta 251 (1996) 273.
[5] M. Westerhausen, T. Bollwein, A. Pfitzner, T. Nilges, H.J. Deiseroth, Inorg. Chim. Acta 312 (2001) 239.
[6] M.G. Davidson, D. Elilio, S.L. Less, A. Martín, P.R. Raithby, R. Snaith, D.S. Wright, Organometallics 12 (1993) 1.
[7] M. Westerhausen, T. Bollwein, P. Mayer, H. Piotrowski, A. Pfitzner, Z. Anorg. Allg. Chem. 628 (2002) 1425.
[8] M. Westerhausen, T. Bollwein, N. Makropoulos, T.M. Rotter, T. Habereder, M. Suter, H. Nöth, Eur. J. Inorg. Chem. (2001) 851.
[9] (a) M. Westerhausen, A.N. Kneifel, P. Mayer, Z. Anorg. Allg. Chem. 632 (2006) 634;
(b) M. Westerhausen, T. Bollwein, N. Makropoulos, S. Schneiderbauer, M. Suter, H. Nöth, P. Mayer, H. Piotrowski, K. Polborn, A. Pfitzner, Eur. J. Inorg. Chem. (2002) 389.
[10] M. Westerhausen, T. Bollwein, K. Karaghiosoff, S. Schneiderbauer, M. Vogt, H. Nöth, Organometallics 21 (2002) 906.
[11] M. Westerhausen, T. Bollwein, M. Warchhold, H. Nöth, Z. Anorg. Allg. Chem. 627 (2001) 1141.
[12] (a) J.T.B.H. Jastrzebski, J.M. Klerks, G. van Koten, K. Vrieze, J. Organomet. Chem. 210 (1981) C49;
(b) G. van Koten, J.T.B.H. Jastrzebski, K. Vrieze, J. Organomet. Chem. 250 (1983) 49;
(c) A.L. Spek, J.T.B.H. Jastrzebski, G. van Koten, Acta Crystallogr., Sect. C 43 (1987) 2006;
(d) E. Wissing, S. van der Linden, E. Rijnberg, J. Boersma, W.J. Smeets, A.L. Spek, G. van Koten, Organometallics 13 (1994) 2602.
[13] (a) N.L. Rosi, J. Eckert, M. Eddaoudi, D.T. Vodak, J. Kim, M. O'Keeffe, O.M. Yaghi, Science 300 (2003) 1127;
(b) J.L.C. Rowsell, A.R. Millward, K.S. Park, O.M. Yaghi, J. Am. Chem. Soc. 126 (2004) 5666;
(c) B. Kesanli, Y. Cui, M.R. Smith, E.W. Bittner, B.C. Brockrath, W. Lin, Angew. Chem., Int. Ed. 44 (2005) 72.
[14] W. Kuran, M. Czernecka, J. Organomet. Chem. 263 (1984) 1.
[15] R.J. Herold, S.L. Aggarwal, V. Neff, Can. J. Chem. 41 (1963) 1368.
[16] S.S. Al-Juaid, N.H. Buttrus, C. Eaborn, P.B. Hitchcock, A.T.L. Roberts, J.D. Smith, A.C. Sullivan, J. Chem. Soc., Chem. Commun. (1986) 908.
[17] S. Jana, R.J.F. Berger, R. Fröhlich, T. Pape, N.W. Mitzel, Inorg. Chem. 46 (2007) 4293.
[18] G. Anantharaman, K. Elango, Organometallics 26 (2007) 1089.
[19] M. Westerhausen, A.N. Kneifel, I. Lindner, J. Grčić, H. Nöth, Z. Naturforsch. 59b (2004) 161.
[20] A. Almenningen, T.U. Helgaker, A. Haaland, S. Samdal, Acta Chem. Scand., Ser. A 36 (1982) 159.
[21] E. Frankland, Justus Liebigs Ann. Chem. 71 (1894) 171.
[22] J. Penner-Hahn, Curr. Opin. Chem. Biol. 11 (2007) 166.
[23] (a) H.J. Zhu, J.X. Jiang, S. Saebo, C.U. Pittman Jr., J. Org. Chem. 70 (2005) 261;
(b) M. Sosa-Rivadeneyra, O. Muñoz-Muñiz, C.A. Anaya de Parrodi, L. Quintero, E. Juaristi, J. Org. Chem. 68 (2003) 2369;
(c) J. Weston, Organometallics 20 (2001) 713;
(d) M. Yamakawa, R. Noyori, Organometallics 18 (1999) 128;
(e) C. Girard, H.B. Kagan, Angew. Chem., Int. Ed. Engl. 37 (1998) 2922;
(f) M. Kitamura, S. Suga, H. Oka, R. Noyori, J. Am. Chem. Soc. 120 (1998) 9800;
(g) B. Goldfuss, K.N. Houk, J. Org. Chem. 63 (1998) 8998;
(h) A. Vidal-Ferran, A. Moyano, M.A. Pericás, A. Riera, Tetrahedron Lett. 38 (1997) 8773;
(i) D.G. Blackmond, J. Am. Chem. Soc. 119 (1997) 12934;
(j) M. Kitamura, H. Oka, S. Suga, R. Noyori, M. Yamakawa, Chem. Eur. J. 2 (1996) 1173;
(k) M. Yamakawa, R. Noyori, J. Am. Chem. Soc. 117 (1995) 6327;
(l) M. Kitamura, S. Suga, M. Niwa, R. Noyori, J. Am. Chem. Soc. 117 (1995) 4832;
(m) M. Kitamura, S. Suga, M. Niwa, R. Noyori, Z.X. Zhai, H. Suga, J. Phys. Chem. 98 (1994) 12776;
(n) K. Soai, S. Niwa, Chem. Rev. 92 (1992) 833;
(o) R. Noyori, M. Kitamura, Angew. Chem., Int. Ed. Engl. 30 (1991) 49;
(p) R. Noyori, S. Suga, K. Kawai, S. Okada, M. Kitamura, N. Oguni, M. Hayashi, T. Kaneko, Y. Matsuda, J. Organomet. Chem. 382 (1990) 19;

(q) M. Kitamura, S. Okada, S. Suga, R. Noyori, J. Am. Chem. Soc. 111 (1989) 4028;
(r) N. Oguni, Y. Matsuda, T. Kaneko, J. Am. Chem. Soc. 110 (1988) 7877;
(s) M. Kitamura, S. Suga, K. Kawai, R. Noyori, J. Am. Chem. Soc. 108 (1986) 6071.
[24] (a) F. Meyer, Eur. J. Inorg. Chem. (2006) 3789;
(b) B. Bauer-Siebenlist, F. Meyer, E. Farkas, D. Vidovic, S. Dechert, Chem. Eur. J. 11 (2005) 4349;
(c) B. Bauer-Siebenlist, F. Meyer, E. Farkas, D. Vidovic, J.A. Cuesta-Seijo, R. Herbst-Irmer, H. Pritzkow, Inorg. Chem. 43 (2004) 4189.
[25] F. Meyer, P. Rutsch, Chem. Commun. (1998) 1037.
[26] E. Jaime, J. Weston, Eur. J. Inorg. Chem. (2006) 793.
[27] (a) E. Jaime, S. Kluge, J. Weston, ARKIVOK iii (2007) 77;
(b) S. Erhardt, E. Jaime, J. Weston, J. Am. Chem. Soc. 127 (2005) 3654.
[28] D. Suarez, E.N. Brothers, K.M. Merz Jr., Biochemistry 41 (2002) 6615.
[29] (a) A.D. Becke, J. Chem. Phys. 98 (1993) 5648;
(b) C. Lee, W. Yang, R.G. Parr, Phys. Rev. B 37 (1988) 785.
[30] M.J. Frisch, G.W. Trucks, H.B. Schlegel, G.E. Scuseria, M.A. Robb, J.R. Cheeseman, J.A. Montgomery Jr., T. Vreven, K.N. Kudin, J.C. Burant, J.M. Millam, S.S. Iyengar, J. Tomasi, V. Barone, B. Mennucci, M. Cossi, G. Scalmani, N. Rega, G.A. Petersson, H. Nakatsuji, M. Hada, M. Ehara, K. Toyota, R. Fukuda, J. Hasegawa, M. Ishida, T. Nakajima, Y. Honda, O. Kitao, H. Nakai, M. Klene, X. Li, J.E. Knox, H.P. Hratchian, J.B. Cross, C. Adamo, J. Jaramillo, R. Gomperts, R.E. Stratmann, O. Yazyev, A.J. Austin, R. Cammi, C. Pomelli, J.W. Ochterski, P.Y. Ayala, K. Morokuma, G.A. Voth, P. Salvador, J.J. Dannenberg, V.G. Zakrzewski, S. Dapprich, A.D. Daniels, M.C. Strain, O. Farkas, D.K. Malick, A.D. Rabuck, K. Raghavachari, J.B. Foresman, J.V. Ortiz, Q. Cui, A.G. Baboul, S. Clifford, J. Cioslowski, B.B. Stefanov, G. Liu, A. Liashenko, P. Piskorz, I. Komaromi, R.L. Martin, D.J. Fox, T. Keith, M.A. Al-Laham, C.Y. Peng, A. Nanayakkara, M. Challacombe, P.M.W. Gill, B. Johnson, W. Chen, M.W. Wong, C. Gonzalez, J.A. Pople, J.A. GAUSSIAN 03, Revision C.02, Gaussian Inc., Wallingford, CT, 2004.
[31] T.H. Dunning Jr., P.J. Hay, in: H.F. SchaeferIII (Ed.), Modern Theoretical Chemistry, vol. 3, Plenum, New York, 1976, p. 1.
[32] (a) P.J. Hay, W.R. Wadt, J. Chem. Phys. 82 (1985) 270;
(b) W.R. Wadt, P.J. Hay, J. Chem. Phys. 82 (1985) 284;
(c) P.J. Hay, W.R. Wadt, J. Chem. Phys. 82 (1985) 299.
[33] (a) E.R. Davidson, Chem. Phys. Lett. 260 (1996) 514;
(b) R.A. Kendall, T.H. Dunning Jr., R.J. Harrison, J. Chem. Phys. 96 (1992) 6796.
[34] M. Westerhausen, B. Rademacher, W. Poll, J. Organomet. Chem. 421 (1991) 175.
[35] G.M. Sheldrick, SHELXL-97, Universität Göttingen, 1997.
[36] D.T. Cromer, J.B. Mann, Acta Crystallogr. 24 (1968) 321.
[37] R.F. Stewart, E.R. Davidson, W.T. Simpson, J. Chem. Phys. 42 (1965) 3175.